Construction and Building Materials 94 (2015) 126–136

Contents lists available at ScienceDirect

Construction and Building Materials

journal homepage: www.elsevier.com/locate/conbuildmat

Bond behaviour of reinforcing bars in cracked concrete

Pieter Desnerck *, Janet M. Lees, Chris T. Morley

Department of Engineering, University of Cambridge, Trumpington Street, CB2 1PZ Cambridge, United Kingdom

HIGHLIGHTS

- A novel method to test bond in cracked reinforced concrete specimens is presented.
- Effect of number of cracks, orientation, confinement and cover is investigated.
- Results indicate a significant loss of bond strength for single cracked specimens.
- Concrete cover and confinement play a significant role.
- Crack orientation with respect to the rib pattern is of minor influence.

ARTICLE INFO

Article history:
Received 9 March 2015
Received in revised form 3 June 2015
Accepted 18 June 2015
Available online 7 July 2015

Keywords:
Bond strength
Corrosion
Pull-out strength

ABSTRACT

Due to the relatively low tensile strength of concrete, cracks are inherent in reinforced concrete structures. A common cause of cracking is the corrosion of internal steel reinforcement, a deterioration process that can affect the bond behaviour and anchorage capacity of reinforcing bars. Corrosion leads to a reduction of the reinforcing bar diameter, the formation of a weak layer of corrosion products around the bar and expansive forces on the surrounding concrete (that can lead to cracking). In the past, the impact of corrosion on bond has been investigated by means of accelerated corrosion tests. However, the more fundamental impact of cracking as distinct from corrosion products on the bond reduction is still not fully understood.

This study applies a novel test method to investigate the bond behaviour of reinforcing bars in cylindrical cracked reinforced concrete specimens. The influence of the number of cracks, crack orientation, confinement and concrete cover are investigated.

The results indicate a significant loss of bond strength for single cracked specimens. This reduction becomes as high as 65% for double cracked specimens in the absence of confinement. It is shown that the crack orientation with respect to the rib pattern is of minor influence, but the concrete cover and confinement play a significant role in the obtained bond characteristics.

1. Introduction

Concrete is an inhomogeneous material with a relatively low tensile strength. Therefore it is often used in combination with steel reinforcement so that the steel can resist tensile stresses after cracking. The load bearing capacity and serviceability performance of reinforced concrete structures depend highly on the interaction between reinforcing bars and the surrounding concrete [1]. Over time the bond can degrade due to deterioration of the reinforcement and/or the surrounding concrete. When cracks develop in regions surrounding the reinforcing bars, the force transfer is affected and this can lead to lower anchorage capacities or an altered bond behaviour.

Cracks are inherent in reinforced concrete structures and are caused by a number of different types of actions [2]. One of the most severe forms of cracking in hardened reinforced concrete structures is the result of the corrosion of steel reinforcing bars. Due to carbonation and chloride ingress a favourable environment is created for corrosion to initiate and corrosion products to be formed [2]. Fib bulletin No. 10 [1] categorises the effects of corrosion into 3 potential consequences:

- loss of reinforcing bar section,
- creation of a weak interfacial layer at the reinforcing bar/concrete interface,
- volumetric expansion of the reinforcing bar.

* Corresponding author.
E-mail addresses: Pieter.Desnerck@eng.cam.ac.uk (P. Desnerck), jml2@eng.cam.ac.uk (J.M. Lees), ctm1@cam.ac.uk (C.T. Morley).

http://dx.doi.org/10.1016/j.conbuildmat.2015.06.043
0950-0618/

Abbreviations and notations

ϕ	reinforcement bar diameter, mm	f_y	yield strength of a reinforcing bar, N/mm^2
σ_s	tensile stress in the reinforcing bar, N/mm^2	F_s	total tensile force in a reinforcing bar, N
τ_M	characteristic value of the bond strength, N/mm^2	k	bond length expressed as 'times the bar diameter ϕ', –
τ_R	ultimate bond strength, N/mm^2	l_d	bond length, mm
BRF	bond reduction factor, –	s_u	slip corresponding to the ultimate bond strength, mm
DEV	standard deviation	RBF	retained bond factor, –
f_c	concrete compressive strength, N/mm^2	w	crack width, mm
$f_{c,cub}$	concrete cube compressive strength, N/mm^2	w_u	ultimate crack width after bond tests, mm
$f_{ct,sp}$	concrete splitting tensile strength, N/mm^2		
f_u	ultimate tensile strength of a reinforcing bar, N/mm^2		

The last two phenomena have a direct influence on the bond of the reinforcing bar. On one hand, a weak interface layer of brittle corrosion products surrounding the reinforcing bar increases the relative displacement of the bar with respect to the concrete at certain load levels. On the other hand corrosion products are expansive in nature and tend to generate tensile stresses in the surrounding concrete. At low levels this expansion may be advantageous but once these stresses exceed the tensile capacity of the concrete, cracks around and along the reinforcing bars develop [1]. The reduction in confinement due to these cracks then leads to a progressive reduction in the bond strength. Hence, understanding of the link between corrosion rates, the induced cracking (and crack widths) and the reduction in bond capacity is essential.

To investigate crack formation due to corrosion, researchers [3–9] have undertaken accelerated corrosion tests on reinforced concrete specimens where impressed currents of 0.003–10 mA/cm^2 were applied. Table 1 summarizes results found in literature on the corrosion levels to cause cracking of the concrete cover (defined by the appearance of visible cracks with a width of 0.03–0.05 mm at the outer surface of the specimens). The corrosion levels are expressed as a percentage of bar cross-sectional area loss (section loss expressed as a uniform metal loss around the circumference of the reinforcing bar) and corrosion penetration depth x radially into the bar. Although there is some scatter in the obtained values, all studies agree that a relatively low corrosion penetration depth, ranging from 0.008 to 0.130 mm, causes cracking.

Rodriguez et al. [3] found that cracks were initiated for corrosion levels associated with bar radius reductions as low as 0.015 mm to 0.040 mm. But the cracking was delayed in specimens with an increased concrete cover and tensile strength. However Andrade et al. [4] reported a negligible effect of cover/bar ratio on cracking.

In previous studies, researchers have tried to link observed crack widths to the degree of corrosion in reinforcing bars. There is no agreed consensus on the exact relationship, but Vidal et al. [10] gathered data from beam tests with different bar diameters to deduce a linear relationship between crack widths w in mm and a loss of steel cross-sectional area of reinforcing bars:

$$w = K \cdot (A_{s0} - A_s) \quad (1)$$

where K is an empirical value of 0.0575 and $(A_{s0} - A_s)$ is the cross-sectional area loss of the reinforcing bar in mm^2.

A similar linear relationship, expressed as a function of the corrosion penetration depth x in mm, was proposed by Rodriguez et al. [3]:

$$w = 0.05 + \beta \cdot x \quad (2)$$

where β is a coefficient depending on the bar position in the element (β = 0.0100 for top bars and 0.0125 for bottom bars).

The bond reduction due to corrosion of reinforcing bars in concrete has also been the subject of investigation over recent decades [5,7,11–16]. Most studies apply accelerated corrosion techniques [17] to achieve a specific state of corrosion before the bond properties are assessed. The obtained results show a significant amount of scatter, but do agree on a bond reduction for significant levels of corrosion. Residual bond strengths of 15–110% are reported for cover ratios c/d ranging from 1.0 to 7.5 and higher, with values above 100% for very low corrosion levels (the initial formation of corrosion products can fill the pore structure around the bar and hence increase the bond strength slightly). The selected results shown in Fig. 1 indicate the lack of a clear relationship between the cover ratio c/d and the retained bond factor (RBF). For more detailed information, reference is made to fib Bulletin No. 10 [1].

One issue with accelerated corrosion bond tests is that they study the combined effect of cracking and the formation of a soft layer of corrosion products around the reinforcement. While these

Table 1
Overview of reported corrosion levels to cause concrete cover cracking.

Study	Bar diameter (mm)	Cover ratio (–)	Section loss (%)	Corrosion penetration x (mm)
Al-Sulaimani et al. [5]	10	7.50	5.00	0.130
	14	5.36	3.00	0.110
	20	3.75	2.00	0.100
Clark and Saifullah [8]	8	0.50–2.00	0.40–1.30	0.008–0.026
Andrade et al. [4]	16	1.25–1.88	0.40–0.50	0.015–0.020
Rodriguez et al. [3]	16	2.00–4.00	0.40–1.00	0.015–0.040
Clark and Saifullah [6]	8	1.00	0.30–0.55	0.006–0.011
Almusallam et al. [7]	12	5.00	4.00	0.120
Alonso et al. [9]	8–16	1.25–7.00	0.19–1.30	0.015–0.065

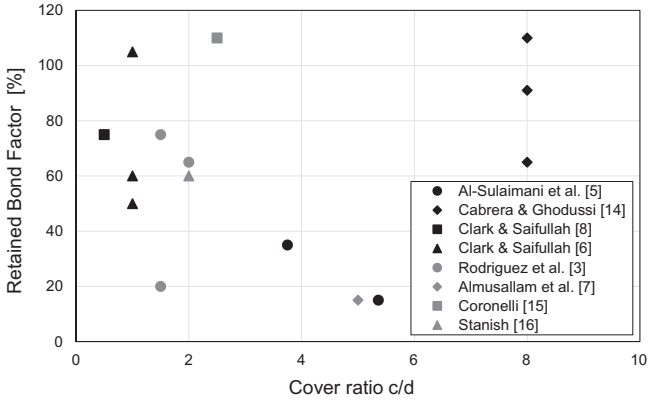

Fig. 1. Relationship between cover ratio c/d and residual bond strength as reported in literature.

effects co-exist in practice, it leads to difficulties in analysing the processes at a fundamental level. Furthermore the results cannot be applied to situations in which cracks are present in the absence of corrosion (e.g. plastic shrinkage cracks in congested reinforcement lay-outs).

This study aims to quantify the bond strength of reinforcing bars in cracked concrete. Rather than performing accelerated corrosion tests, it focuses on the more fundamental effect of the cracking itself (in absence of corrosion products). To achieve this aim, a novel test method is developed.

2. Crack generation

When assessing existing structures, engineers often observe severe cracking due to corrosion. Depending on the location of the reinforcing bar within the structure, the crack orientation and extent can differ, which in turn can influence the bond properties. Some common corrosion induced crack patterns are shown in Fig. 2.

As discussed, most studies on the bond properties of cracked concrete specimens have used accelerated corrosion techniques. However, these techniques have the tendency to lead to less controllable crack patterns and a wide range of obtained crack widths. Gambarova et al. [18] studied the bond of reinforcing bars in pre-cracked specimens. The cracks were formed by applying a transverse tensile force on a specially designed concrete element (steel shoulders with shear pins were cast into the specimen to allow for the application of the force). The specimens were relatively large and the test set-up consisted of external confinement provided by a 'confinement cell'. In research projects focussing on diffusion of contaminants in concrete, cracks are often introduced in one of the following ways: artificially by using thin inserts (e.g. metal sheet) [19], 3-point bending tests, wedge splitting tests [20], mechanical expansive cores [21] or controlled splitting tests [22]. As with respect to bond tests, use of inserts (eliminating the aggregate interlock between the crack faces), wedge shaped specimens or an expansive core are not easy to implement and are not necessarily representative of cracked concrete.

In this study the principles of a controlled split tensile test are applied to pre-crack specimens. In this way rough crack surfaces are then formed along a predefined cracking plane running through the axis of the reinforcing bar. To avoid brittle failure and provide some post-cracking confinement, the specimen can be cast within a plastic ring. This ring can remain in place during both the pre-cracking and pull-out phases. Singly reinforced cylindrical specimens are well suited to split tensile tests. With this technique, single or double cracks can be generated to represent observed crack patterns in existing structures.

Of particular interest are the bond reductions during the early stages of corrosion and thus the onset of cracking. Based on Eqs. (1) and (2), a 1% loss of steel section corresponds to crack widths of about 0.03–0.04 mm, therefore the splitting tests seek to achieve similar values. These crack widths are relatively small compared to the allowable crack widths of 0.20–0.30 mm according to reinforced concrete design guidance [23].

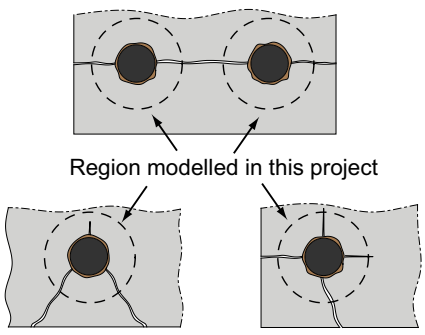

Fig. 2. Possible cracks patterns in reinforced concrete due to corrosion.

3. Experimental program

3.1. Experimental specimens and overview of test method

In order to represent common crack patterns (as illustrated in Fig. 2) and determine the bond strength of reinforcing bars in cracked, the proposed test method includes one or two pre-cracking phases followed by standard bond strength "pull-out tests" [24].

In the pre-cracking phase(s) the specimens are subjected to a split cylinder test. Two line loads are applied on the specimen on opposite sides and along the axis of the concrete cylinder until first cracking of the concrete, at which point the specimen is unloaded. For double cracked specimens, the specimen is rotated 90° after the first pre-cracking experiment and the same procedure is repeated to induce the second crack. Pull-out tests are then conducted on the cracked specimens to determine the influence of the cracks on the bond behaviour. The test procedure is shown schematically in Fig. 3.

Cylindrical specimens with a diameter of either 107 mm or 60 mm, and a height of 100 mm are used. A reinforcing bar with a diameter of 10 mm is centrally placed in the specimen, resulting in a cover-to-diameter ratio of 4.8 or 2.5. The prescribed bond length for pull-out tests according to RILEM recommendations [24] is 10 times the bar diameter ϕ. However, as shown in other studies [25–27], this can lead to yielding and in some cases the rupture of the reinforcement bar before reaching the ultimate bond strength. Therefore the specimens are cast with a bond length of 5 times the bar diameter. The bond length itself is reduced by providing a sleeve over the bar in the lower 50 mm (Fig. 4). The specimens are cast in a plastic cylindrical mould which is used as confinement for the specimen during the pre-cracking phases and in many cases also remains in place for the pull-out tests (the plastic confinement is not removed at the time of demoulding).

In order to be able to install measuring devices on the passive side (free end of the bar), the reinforcing bar extends 100 mm beyond the concrete surface. At the active end the reinforcing bar extends 400 mm beyond the concrete to provide room for sensors and provide a sufficient length to grip the bar in the clamps of the testing machine.

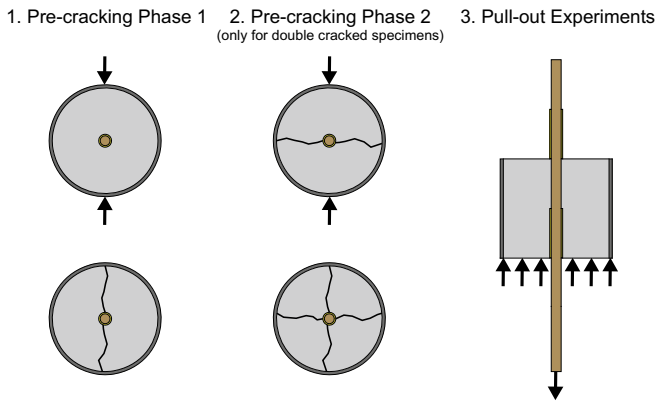

Fig. 3. Test procedure.

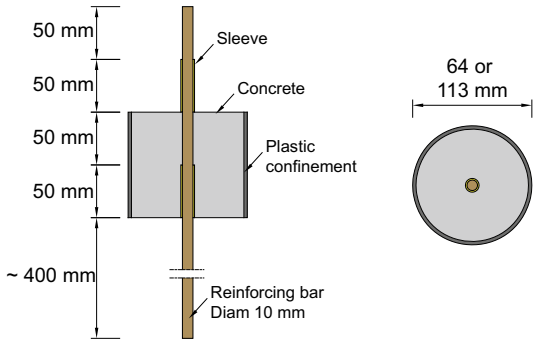

Fig. 4. Specimen geometry.

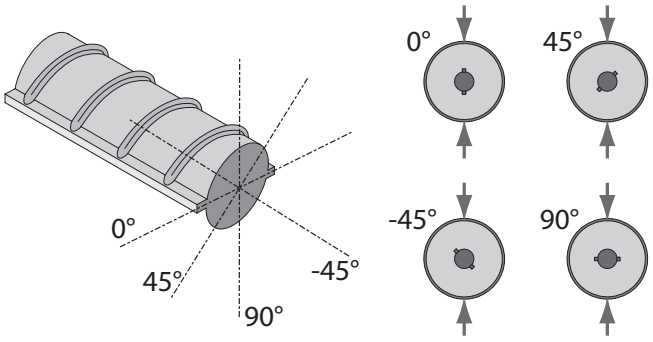

Fig. 5. Applied crack orientations with respect to the reinforcing bars rib pattern.

3.2. Main parameters

The following parameters were selected for investigation: single or double pre-cracks (number of cracks), the crack orientation relative to the reinforcing bar rib pattern, the confinement and the concrete cover.

As reinforced concrete structures are currently primarily constructed with ribbed reinforcing bars, the crack itself can cross the rib pattern of the bar at different angles (see Fig. 5). Cracks running along the longitudinal ribs, leaving the concrete around the transverse rib intact, might have a less detrimental impact on the bond compared to cracks that hit the transverse ribs. Whether this crack angle influences the bond behaviour is currently unknown.

Crack widths are often governed by the amount of transverse reinforcement. For longitudinal cracks running along the longitudinal reinforcing bars, the transverse reinforcement provides a form of confinement transferring forces from one crack face to another and reducing the crack width. As more confinement is provided, the hoop stresses induced during pull-out of a longitudinal reinforcing bar might be counteracted and in this way provide sufficient resistance for the anchorage force to build up [28]. However, if the confinement is limited these hoop stresses can lead to the cracks opening up and a decrease in the bond properties.

Similar to the confinement provided by transverse reinforcement, the concrete cover can also provide confinement. Increasing the concrete cover leads to a bigger influence zone around the reinforcing bar that can resist hoop stresses and thereby increase the bond strength of the bar.

3.3. Test series

A total of four series of experiments are undertaken. Each series consists of 4 sets of 5 identical specimens. In this way five individual results are obtained for each parameter combination. The entire test matrix for the total of 80 tests carried out is shown in Table 2.

In Series 1 the angle of a single crack with respect to the rib pattern of the bar is varied. Different angles are achieved through different orientations of the specimens relative to the applied split tensile load (Fig. 5). In addition to a reference uncracked set, a single cracked set with crack angle of 0°, 45° and 90° is tested. The crack angle itself is measured with respect to the plane running through the bar axis and the longitudinal ribs (see Fig. 5).

Series 2 focusses on double cracked specimens where the crack orientation relative to a reference plane through the bar axis and longitudinal ribs varies. A reference set, a set with cracks orientated at 0° and 90° relative to the reference plane, and a set with −45° combined with 45° cracks are tested. As the cracks are formed by applying a splitting test, the crack faces of the first crack are compressed during the second splitting phase. To investigate the potential influence of this sequence, a fourth set of specimens was included. Instead of pre-cracking in the 0° direction (as in set 2-B), in set 2-D the first crack was applied at 90° followed by the one at 0°. In this way, the predominant crack (with the biggest crack width) in set 2-D was the one perpendicular to the longitudinal ribs, whereas in set 2-B it was the one parallel to the longitudinal ribs.

Table 2
Overview of parameter combinations for the tested specimen series.

Series	Set	Confinement		Diameter (mm)		Single crack angle			Double crack angle		
		No	Yes	60	107	0	45	90	0 and 90	−45 and 45	90 and 0
1	A		X		X						
	B		X		X	X					
	C		X		X		X				
	D		X		X			X			
2	A		X		X						
	B		X		X				X		
	C		X		X					X	
	D		X		X						X
3	A	X			X						
	B	X			X	X					
	C	X			X			X			
	D	X			X				X		
4	A		X	X							
	B		X*	X*	X*	X					
	C		X	X		X					
	D		X	X					X		

* Pre-cracked specimen of 60 mm cast in a 107 mm specimen

Series 3 consisted of specimens where the plastic tube confinement was removed after the cracking phase. The different parameter combinations tested without confinement are uncracked reference specimens, single cracked specimens with cracks orientated at either 0° or 90° to the reference plane and a set of double cracked specimens with a crack at 0° combined with a crack at 90°.

In the last series, Series 4, the concrete cover was reduced by casting the specimens in a cylindrical tube with an inner diameter of only 60 mm, reducing the original cover by 23 mm and resulting in a cover-to-diameter ratio of 2.5. An uncracked reference set, a set of specimens with single crack (crack angle 0°) and a set of double cracked specimens (0° combined with 90°) are tested. The final set in the series consisted of specimens of diameter 60 mm single cracked at 0° after which the plastic confinement was removed. The specimen was then placed in the centre of a 107 mm diameter plastic tube and concrete was cast in the annulus between the specimen and the tube. As a result a 23 mm thick concrete ring was formed around the cracked specimen. This scenario simulates a situation in which the crack starts to grow around the rebar but does not yet extend to the outer surface.

3.4. Materials

A concrete with a 28-day cube compressive strength of about 30 MPa is selected for the tests. The water-to-cement ratio of the mixture is 0.6 and the sand-to-aggregate ratio is 0.45. The concrete is made with an early-strength Portland cement with limestone, type CEM II/A LL 32.5 R [29]. The aggregates are a natural sand with a maximum grain size of 4 mm and specific gravity of 2.65 and a gravel with maximum grain size of 10 mm with specific gravity of 2.65. The mix proportions are summarized in Table 3.

The mixtures are prepared in batches of 40 L from which approximately 20 L are used for the pull-out specimens and the other 20 L for standard concrete control specimens. After 1 min mixing of the dry materials, water is added and mixing continues for 3 min.

After casting, the specimens are stored in standard lab conditions (temperature of 22 ± 2 °C and relative humidity of 70 ± 5%). After 24 h the control specimens are demoulded and stored under water at a temperature of 20 ± 2 °C. The pull-out specimens are taken from the formwork (without removing the plastic confinement rings), wrapped in plastic and stored in standard lab conditions.

The compressive and tensile strengths of the concrete are determined at 21 days (time of pre-cracking) and 28 days (time of bond tests). For the determination of the compressive strength, cubes with sides of 100 mm ($f_{c,cub}$) and cylinders with a height of 200 mm and a diameter of 100 mm (f_c) are used. The splitting tensile strength $f_{ct,sp}$ is measured from cylinders with a diameter of 100 mm and a height of 200 mm. The mean results for the four series are summarized in Table 4.

For the test program, the nominal steel bar diameter is fixed at 10 mm (actual measured value was 9.92 mm). The yield stress f_y and ultimate tensile strength f_u of the high-strength hot-rolled reinforcing bars, are measured in the laboratory as 520 MPa and 606 MPa respectively. The stress–strain diagram is given in Fig. 6(a).

Table 3
Concrete composition.

Constituent	Density (kg/m^3)	Quantity (kg/m^3)
Water	1000	180
Sand	2625	835
Coarse aggregate	2625	1015
CEM II/A LL 32.5 R	3100	300

Table 4
Concrete properties.

Series	$f_{c,cub}$ (MPa)		f_c (MPa)		$f_{ct,sp}$ (MPa)
	21 days	28 days	21 days	28 days	21 days
1	29.5	31.3	22.8	23.3	2.4
2	29.0	30.5	20.0	20.0	2.6
3	25.3	27.6	20.2	22.5	2.5
4	28.4	29.0	23.4	23.8	2.7

All reinforcing bars have the same rib pattern (see Fig. 7) which consist of two longitudinal ribs at opposite sides of the bars and two series of transverse ribs. The rib pattern is measured in the laboratory using a laser measuring device. The transverse ribs are parallel, at 48° to the longitudinal ribs, and of maximum rib height 0.75 mm.

The confinement consisted of a plastic tube with an outer diameter of 113 mm with a wall thickness of 3.2 mm or a tube with a diameter of 64 mm and a wall thickness of 2.1 mm. The stress–strain behaviour of the HDPE plastic was measured in a tensile test set-up, using a dog-bone specimen with a width of 20 mm (the specimen was cut from the plastic tube). The stress–strain response of HDPE is highly dependent on the applied strain rate [30]. As the strains in the confining ring during the bond pull-out test are being built up slowly, a low strain rate of 5×10^{-5} was applied during the material characterisation tests. The obtained results are shown in Fig. 6(b). Both tube diameters showed a similar behaviour under tensile loads.

3.5. Test procedure and instrumentation

At an age of 21 days the specimens are subjected to a split cylinder test according to EN12390-6 [31] (Fig. 8). The test is performed in a rigid load frame with a capacity of 150 kN. A constant deformation rate of 0.4 mm/s is applied until first cracking, at which point the specimen is unloaded. During the splitting test, the applied force as well as the strain on the surface of the plastic tube is recorded. The tube confining strain is measured with strain gauges on opposite sides of the specimens at mid-height.

The obtained crack width is measured using a crack microscope with an accuracy of 0.01 mm at both sides of the reinforcement bar at a distance of 30 mm from the rebar in case of 107 mm specimens and at 20 mm for specimens with a diameter of 60 mm.

The pull-out tests are performed at 28 days in a 150 kN closed loop tensile load frame. The concrete is supported by a steel plate during the test while a tensile force is applied on the reinforcing bar. During the pull-out tests, the specimens are loaded at a constant displacement rate of 0.04 mm/s until a total relative displacement between the tested reinforcing bar and the surrounding concrete of at least 12.5 mm is reached.

The slip of the bar, at the passive as well as the active side, is recorded using 2 sets of 2 linear variable differential transducers (LVDT). These LVDT's are secured to the bar by means of a steel collar mounted to the reinforcing bar (Fig. 9).

After unloading of the specimens the crack widths are measured again.

4. Results and discussion

4.1. Pre-cracking of the specimens

For the pre-cracking stage, the measured applied forces at first cracking induce splitting stresses, calculated based on the principles of standard splitting tensile tests, of around 2.3 MPa (DEV = 0.2 MPa). These splitting strengths are, due to the presence of the reinforcing bar in the splitting plane, slightly lower than the

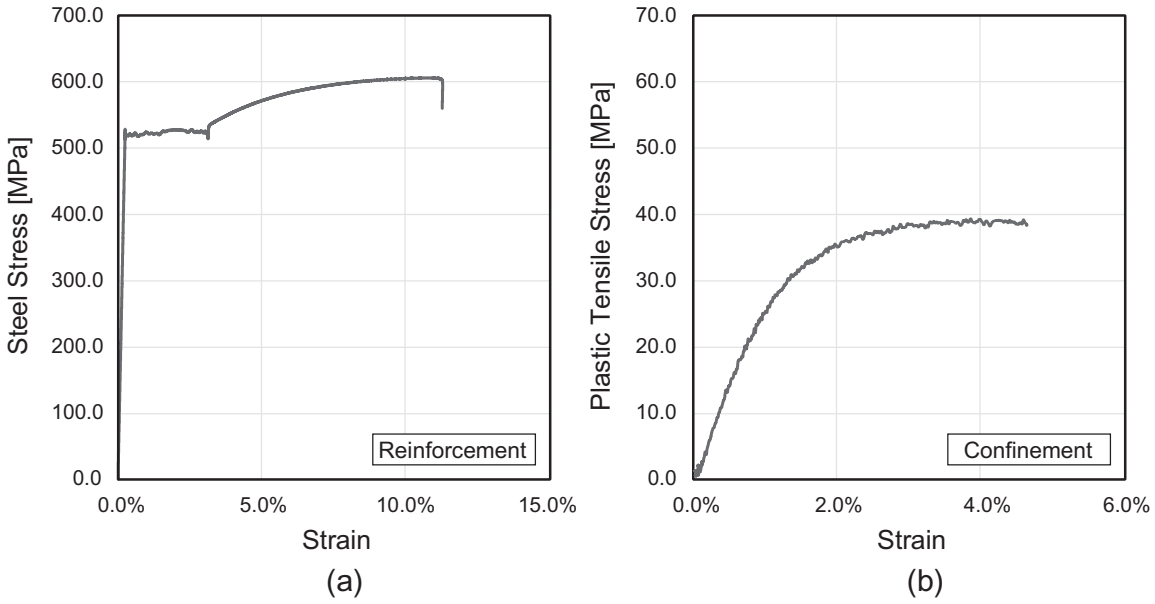

Fig. 6. Stress–strain curves of (a) steel reinforcement bar (diam. 10 mm) and (b) HDPE plastic confinement.

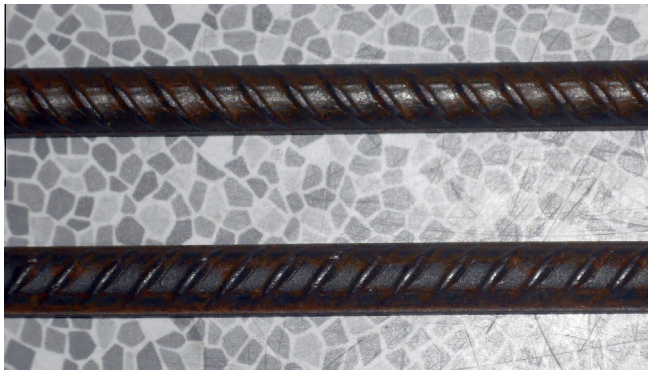

Fig. 7. Rib pattern of reinforcing bars diameter 10 mm.

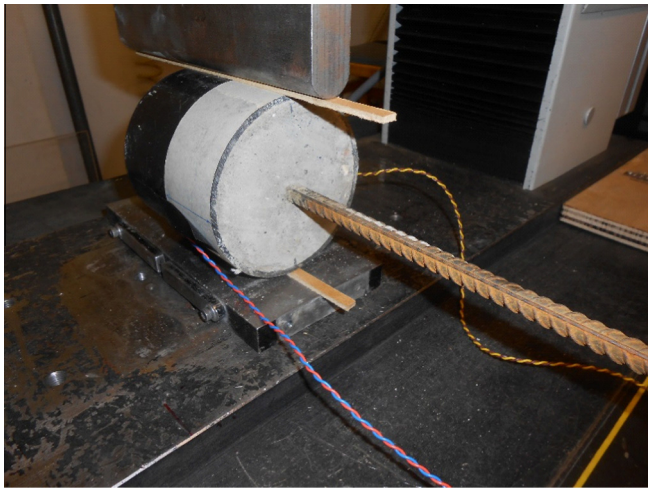

Fig. 8. Instrumentation and test set-up for the pre-cracking phase.

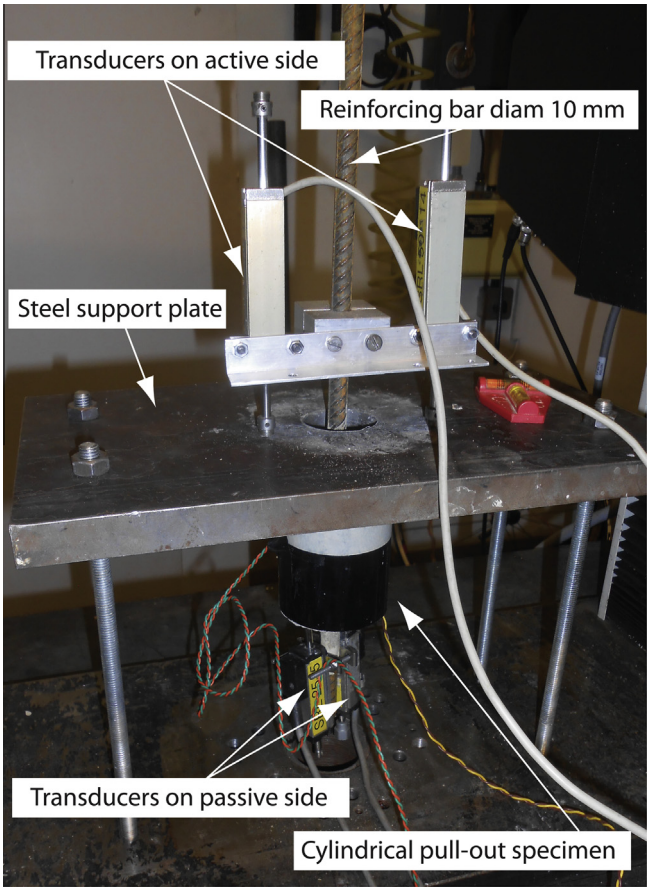

Fig. 9. Instrumentation and test set-up for the pull-out experiments.

tensile splitting strengths measured on standard cylindrical concrete specimens.

Fig. 10 shows one of the measured splitting stress – confinement strain responses for a Series 1 – set B, C and D specimen (single crack oriented at either 0°, 45° or 90° relative to the longitudinal rib). The responses of the other specimens are comparable. As the splitting stress builds up, small compressive stresses are measured in the plastic confinement up until the point where cracking occurs. Thereafter the circumferential strains increase abruptly and become tensile. The final strain in the confinement

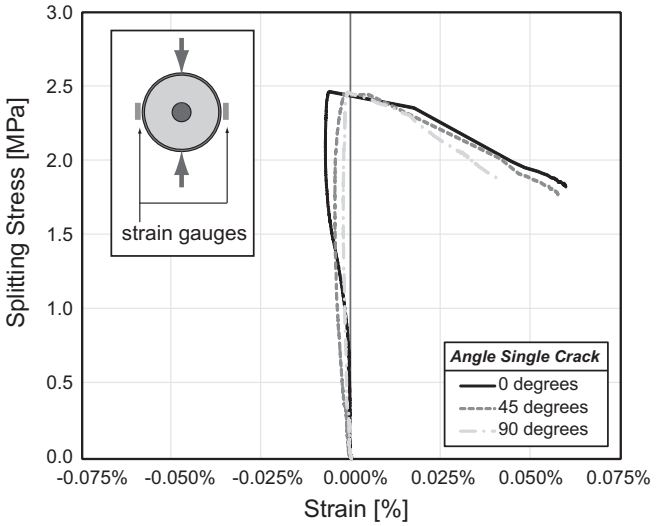

Fig. 10. Confinement strains during pre-cracking tests for single cracked specimens.

after cracking is in the 0.04–0.06% range which corresponds (based on the measured stress–strain diagram) to confinement stresses of 1.8–2.3 MPa in the plastic confinement ring.

The crack widths w after splitting for the pre-cracked specimens are shown in Fig. 11 for the different series and sets. The obtained values are around 0.03 mm but there is significant scatter. Although cracks were visible for all specimens, the 95% confidence intervals of some sets (indicated by the error bars in the figure) included 0.00 mm crack widths. This is due to scatter values of around 0.02 mm for these specific sets. For the double cracked specimens (Series 2) the average of the two (phase 1 and phase 2) obtained crack widths is plotted. Fig. 12 shows the crack patterns for a typical single and double cracked specimen as well as for a single cracked specimen that is then re-cast in a concrete ring. All crack patterns obtained for specimens within the same parameter combination were comparable. No anomalies were detected.

5. Bond strength

From the pull-out experimental results, values of the bond stress can be derived. Assuming a uniform stress distribution along the short bond length, the force F_s in the reinforcing bar is transferred to the concrete over the embedment length l_d resulting in mean bond stresses τ_d of:

$$\tau_d = \frac{F_s}{l_d \cdot \pi \cdot \phi} = \frac{\sigma_s}{4 \cdot k}$$

where σ_s the tensile stress in the reinforcing bar and l_d as a parameter equal to k multiplied by the bar diameter ϕ ($k{\cdot}\phi$).

Two values are of particular interest: the ultimate bond strength τ_R and the often used characteristic bond strength τ_M as defined by RILEM [24]. The ultimate bond strength is defined as the bond stress corresponding to the ultimate load recorded during testing. The characteristic bond strength τ_M is calculated as the mean value of the bond stresses corresponding to a slip of 0.01 mm, 0.10 mm and 1.00 mm.

The slip at the ultimate bond strength s_u is of interest with respect to the ductility of the bond failure.

Table 5 summarizes the obtained results for the different series and sets. The highest ultimate bond strengths are recorded for the reference uncracked specimens, as was to be expected. The three sets of 107 mm diameter reference specimens (c/d = 4.8) all gave ultimate bond strengths of about 19.2 MPa (DEV = 1.4 MPa). The bond strength of the bars tested with a smaller cover (c/d = 2.5 for the 60 mm diameter specimens), turned out to be 14.3 MPa (DEV = 0.8 MPa) as the dominant failure method in this case was a splitting failure (due to the limited reinforcement cover). The ultimate bond strengths of the pre-cracked specimens were all lower than the equivalent reference specimens. The same observations can be made for the characteristic bond strength.

In the analysis hereafter the results of the bond stresses and strengths will be expressed in terms of a retained bond factor (RBF). This factor is defined as the ratio of the actual strength of a specific set to the mean bond strength of the uncracked reference specimens (mean value of all results from sets 1-A, 2-A and 3-A). In this way direct comparisons of the test results within and between

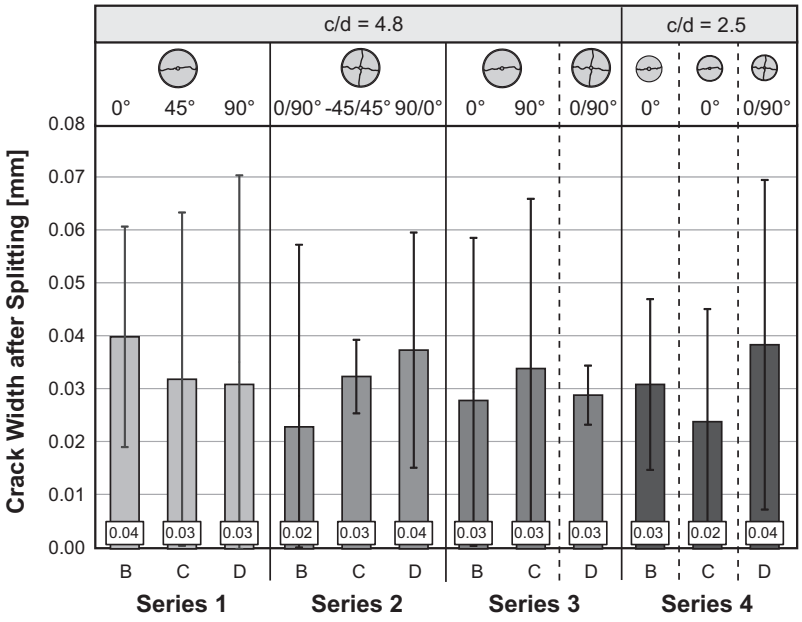

Fig. 11. Crack widths w after pre-cracking phase.

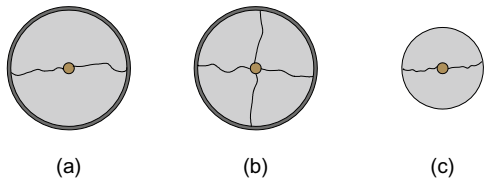

Fig. 12. Observed crack pattern for a typical (a) Series 1B, (b) Series 2B and (c) Series 4B specimen.

series can be made. The bond reduction factor (BRF) can be obtained from the retained bond factor as follows:

$$BRF = 1 - RBF$$

5.1. Crack orientation

The influence of the crack orientation in single cracked specimens was investigated in Series 1. Three different crack angles were considered, 0°, 45° and 90°, with respect to the longitudinal ribs. The results clearly show that the obtained bond strengths are all lower than the reference bond strength (Fig. 13). A *t*-test with a significance level of 95% confirmed this difference to be significant. The differences between the studied crack angles is small and statistically insignificant. Therefore it can be concluded that the orientation of the crack relative to the longitudinal rib has little to no effect on the bond strength. The presence of a single crack however results in a significant reduction in the ultimate bond strength of 44% (RBF = 0.56) for the tested specimens. Those values are slightly higher than the retained bond factors reported earlier (see Fig. 1) for specimens with c/d equal to about 4–5. However, when a wider range of concrete covers is considered, a value for the retained bond factor of 0.56 is well within the reported range of 0.15–1.10.

5.2. Multiple cracks

As was the case for the single cracked specimen, the orientation relative to the longitudinal rib is insignificant, as the 0–90° and −45–45° double cracked specimens gave similar results. In both series the cracks led to ultimate bond strengths that are 54% lower than the uncracked specimens (RBF = 0.46).

The similarity of the set 2-B and 2-D results (double crack with angles 0° and 90°, and 90° and 0°, resp.) suggests that the order in which the cracks were formed also had little effect on the bond performance, as was to be expected from the results of the crack orientation tests. In comparison to the single cracked specimens, the double cracks tend to provide an additional reduction in bond strength of about 10%.

5.3. Confinement

The cracked specimens tested without confinement all tended to fail due to splitting of the specimen rather than a pure pull-out failure as was the case for the other sets. As the ultimate bond strength is reached, the crack width increases drastically leading to a relatively brittle failure of the bond and hence a sudden decrease in the bond stresses with increasing slips. The larger ultimate crack widths w_u associated with this behaviour are evident from the results shown in Table 5.

The unconfined reference specimens provided similar bond strengths to equivalent confined specimens. As the bond failure for both sets was a pure pull-out failure this was to be expected. No cracks were observed on the outer surface of the concrete.

The beneficial effect of the confinement has been reported in earlier studies by Gambarova et al. [18] and is confirmed in this experimental program. The absence of any external confinement further reduces the bond capacity of the 10 mm reinforcing bars. For single cracked specimens, an additional reduction of 11% is measured whereas for the double cracked specimens this reduction is 20%.

5.4. Concrete cover

As the concrete cover is reduced in Series 4 to a cover-to-diameter ratio of 2.5, the failure mode of the reference specimens shifts from a pull-out failure to a splitting failure, hence a reduction in the ultimate bond strength from 19.2 to 14.2 MPa. The single cracked and double cracked specimens show a reduction relative to the reference of 25% (RBF = 0.75) and 41% (RBF = 0.59) respectively, which is slightly less than for the counterparts with a 4.8 cover-to-diameter ratio. This difference can be attributed to the changed failure mode.

For the specimens which originally have a cover-to-diameter ratio of 2.5 on pre-cracking, but are recast to give a cover-to-diameter ratio of 4.8, an increase in bond strength is

Table 5
Experimental results of pull-out test.

Series	Set		τ_R (MPa)		τ_M (MPa)		s_u (mm)		w_u (mm)	
			Mean	DEV	Mean	DEV	Mean	DEV	Mean	DEV
1	A	Reference	20.2	1.3	11.0	0.9	0.95	0.09	0.00	0.00
	B	Single	11.4	0.4	5.5	0.3	0.56	0.09	0.16	0.06
c/d = 4.8	C		11.5	0.5	6.1	0.3	0.58	0.11	0.19	0.06
Confined	D		11.1	0.6	5.6	0.2	0.57	0.10	0.18	0.08
2	A	Reference	19.6	1.0	11.1	1.4	0.89	0.09	0.00	0.00
	B	Double	8.7	0.6	4.0	0.4	0.65	0.13	0.08	0.04
c/d = 4.8	C		9.5	0.6	4.3	0.4	0.63	0.12	0.07	0.01
Confined	D		9.0	0.8	4.4	0.5	0.69	0.13	0.07	0.03
3	A	Reference	17.9	0.9	10.3	1.0	0.92	0.14	0.00	0.00
	B	Single	8.0	0.7	2.9	0.4	0.41	0.12	2.02	0.70
c/d = 4.8	C		8.1	1.0	3.4	1.0	0.54	0.12	1.62	0.49
Unconfined	D	Double	6.4	1.2	2.3	0.6	0.38	0.05	0.89	0.37
4	A	Reference	14.3	0.8	8.2	1.1	0.45	0.23	0.12	0.03
	B*	Single	16.1	0.6	9.3	1.7	0.43	0.24	0.36	0.59
c/d = 2.5	C	Single	10.6	0.9	7.1	1.5	0.31	0.12	0.13	0.01
Confined	D	Double	8.4	0.9	4.5	0.6	0.61	0.20	0.08	0.02

* Re-cast = specimen with c/d = 2.5 pre-cracked and re-casted to achieve c/d = 4.8.

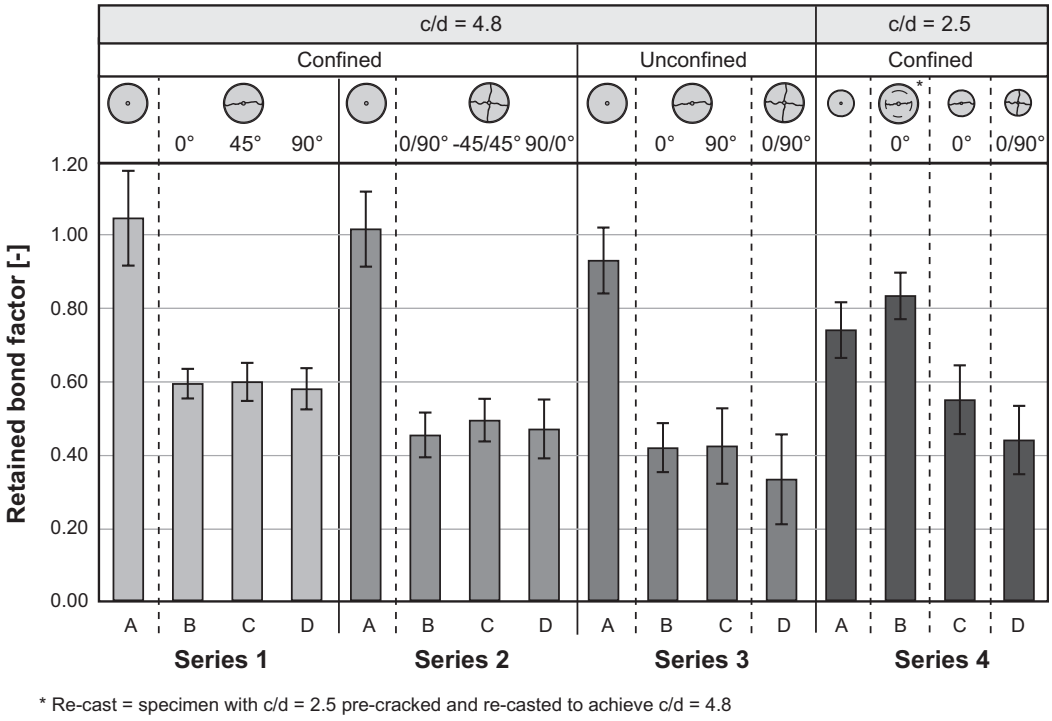

Fig. 13. Bond reduction with respect to uncracked reference specimens.

measured. Compared to the original uncracked specimens with a c/d-ratio of 2.5, the increase is 21%. The concrete ring with a thickness of 23 mm is sufficient to carry the hoop stresses built up during the pull-out test and hence prevent a splitting failure. Failure in these specimens occurs due to pull-out. The cracks in the inner cylinder do not extend to the surface of the uncracked concrete. Comparing these specimens to the original specimens with a cover-to-diameter ratio of 4.8, shows that the re-cast specimens are stronger than the single cracked specimens. This suggests that the bond strength is less affected by partial cracking than in the case where the cracks extend to the outer surface of the concrete. However, the bond strength is lower than measured for uncracked reference specimens with $c/d = 4.8$.

5.5. Implications for design

Current guidelines and standards take into account the effects of micro-cracking, small voids underneath reinforcing bars, potential light forms of corrosion, etc. by applying a relatively high safety factor on design bond strengths. The design implications of the experimental observations of a reduced bond strength due to cracking have not yet been fully identified. More work is required to relate the values obtained in this study to design values, as those might already – perhaps without explicitly realising it – allow partially for the effect of cracks along the bar.

6. Bond stress – slip relationship

During the pull-out tests, the relative displacement between the reinforcing bar and the surrounding concrete is measured so the bond stress–slip relationship can be plotted.

For a given set of 5 specimens, the results show a high repeatability as illustrated in Fig. 14 for Series 1-B (single cracked specimens with cracks at 0°). The measurements on the passive side

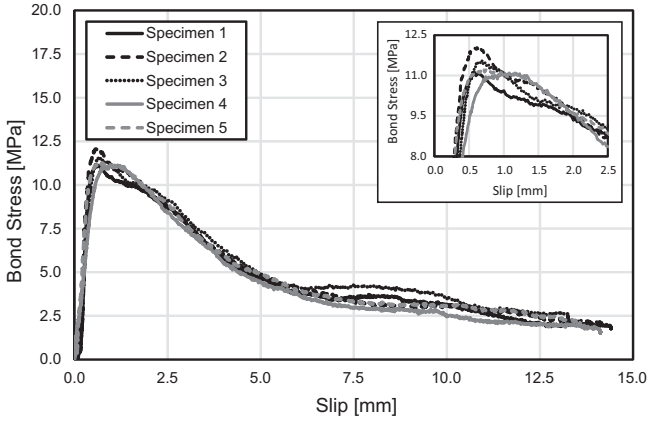

Fig. 14. Bond stress – slip diagram for single cracked specimens with cracks angles of 0° (Series 1 B).

gave similar slip values to those measured on the active side after correction for the linear elastic deformation of the reinforcing bar.

As stated previously, the crack orientation does not significantly influence the obtained characteristic or ultimate bond strength. A comparison of the bond stress – slip diagrams obtained for 0°, 45° or 90° crack angles (Fig. 15), confirms that the crack orientation relative to the reinforcing bars longitudinal rib has little to no influence on the bond response.

A plot of the bond stress–slip response of a typical uncracked, single cracked and double cracked specimen shows that the slope of the initial ascending branch decreases with an increasing number of cracks (Fig. 16), indicating a decrease in stiffness. As the bond stresses increase, the slip seems to increase in an almost linear way. As soon as the ultimate bond strength is reached however, a steeper descending curve is measured for uncracked specimens when compared to single or double cracked ones. Thereafter, the bond stresses

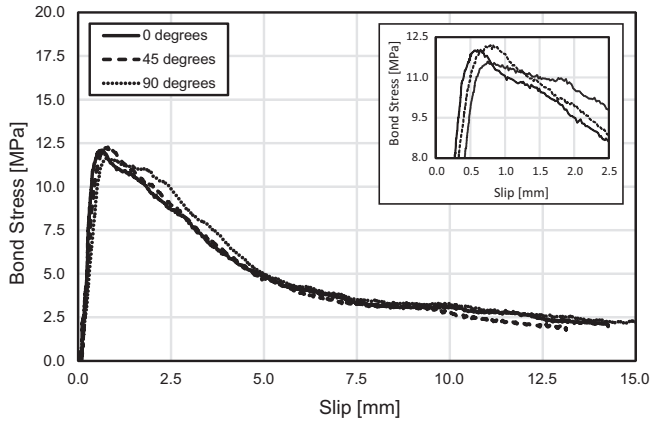

Fig. 15. Influence of crack angle on the bond stress – slip diagram for single cracked specimens.

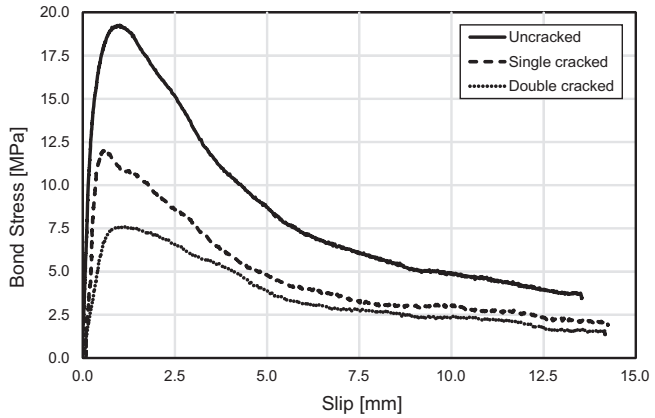

Fig. 16. Influence of the number of cracks on the bond stress – slip diagram.

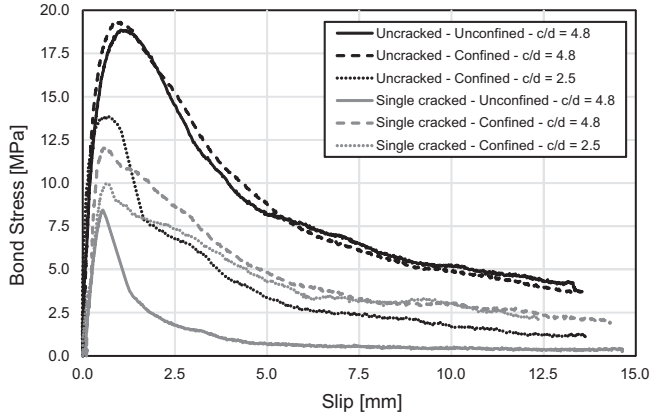

Fig. 17. Influence of confinement on the bond stress – slip diagram.

recorded for higher slip values decrease with an increasing number of cracks, indicating not only the ultimate strength, but also the post-failure behaviour is influenced by the cracks.

The bond stress – slip behaviour of the uncracked reference specimens is not influenced by the plastic tube for the higher concrete cover ratio c/d of 4.8 (Fig. 17). In contrast, for single cracked specimens, the confinement has a significant impact on the bond behaviour. With respect to the recorded slips, a sudden drop in bond stress is noticed for small slip increments beyond the ultimate bond strength. Hence a more sudden bond degradation is noted due to opening up of the cracks as shown by the measured w_u values when there is no confinement. Reducing the concrete cover in a single cracked confined specimen has an effect, but the overall shape is comparable and the post-peak behaviour beyond a slip of approximately 5 mm is similar.

7. Conclusion

Reinforcement corrosion can result in a severe form of concrete cracking. As cracks due to corrosion run along the concrete – rebar interface, the force transfer between the two materials, and more specifically the bond behaviour, is influenced.

To study the effect of the crack angle (relative to a plane running through the axis of the bar and the longitudinal ribs), extent of cracking, confinement and cover depth on the bond properties of reinforcing bars embedded in concrete, an experimental test program was conducted. Cylindrical specimens with a central 10 mm diameter reinforcing bar and a compressive strength of 25 MPa were pre-cracked by applying split tensile forces. Pull-out tests were then carried out on the cracked specimens to determine the bond properties. The results of the tests indicated that:

(1) The presence of cracks, even with minor crack widths of 0.03–0.04 mm, result in a significant reduction of the bond strength. For specimen with a single crack the reduction was on average 44% and for double cracked specimens the reduction was 54%. The measured values for single and double cracked specimens are within the relatively wide range of values reported by other researchers in the past.
(2) The crack orientation with respect to the rib pattern of the reinforcing bars has little or no effect on the obtained bond properties. Three different crack orientations were tested and the results showed similar ultimate bond strengths.
(3) For double cracked specimens the order in which the cracks are formed (linked to the test method) has no significant influence on the bond behaviour.
(4) Confinement influences the ultimate bond strength of a pre-cracked specimen. In the absence of a restraining force, existing cracks can open up fully enabling the reinforcing bar to more easily slip out of the specimens. The reduction of bond capacity between confined and unconfined specimens was an additional 11% for a given parameter combination.
(5) When the concrete cover is reduced, the residual bond strength after cracking is reduced as well. For smaller covers the failure mode of the uncracked concrete shifts from a pull-out failure to a splitting failure.
(6) The bond strength of reinforcing bars in cracked cylinders embedded in an uncracked concrete ring of 23 mm is 18% lower than uncracked specimens with the same total concrete cover. However, the obtained values are higher than those obtained for concrete with a single crack extending through the entire concrete cover but confined by a plastic tube of 2.1 mm thick.

The obtained test results indicate that the presence of longitudinal cracks can significantly influence the bond behaviour of ribbed reinforcing bars in concrete. This suggests that bond reduction factors are necessary for cracks that run along the reinforcement bars when undertaking load bearing capacity checks of existing reinforced concrete structures.

Acknowledgements

The authors would like to gratefully acknowledge the financial support of the UK Engineering and Physical Sciences Research Council (EPSRC) through the EPSRC Project 'Reinforced concrete half-joint structures: Structural integrity implications of reinforcement detailing and deterioration' [Grant no. EP/K016148/1].

Additional data related to this publication is available at the University of Cambridge's institutional data repository: https://www.repository.cam.ac.uk/handle/1810/248740.

References

[1] Task Group Bond Models, fib Bulletin 10 – Bond of Reinforcement in Concrete, Lausanne, 2000.
[2] BRE Centre for Concrete ConstructionCorrosion of steel in concrete – durability of reinforced concrete structures, Digest 444 (2000) 12.
[3] J. Rodriguez, L. Ortega, A. Garcia, Assessment of structural elements with corroded reinforcement, in: Proceedings of the International Conference on Corrosion and Corrosion Protection of Steel in Concrete, 1994, pp. 171–185.
[4] C. Andrade, C. Alonso, F. Molina, Cover cracking as a function of bar corrosion: part I-experimental test, Mater. Struct. 26 (1993) 453–464.
[5] G. Al-Sulaimani, M. Kaleemullah, I. Basunbul, Influence of corrosion and cracking on bond behavior and strength of reinforced concrete members, ACI Struct. J. 87 (2) (1990) 220–231.
[6] L. Clark, M. Saifullah, Effect of corrosion rate on the bond strength of corroded reinforcement, in: Proceedings of the International Conference on Corrosion and Corrosion Protection of Steel in Soncrete, 1994, pp. 591–602.
[7] A. Almusallam, A. Al-Gahtani, R. Abdur, Rasheeduzzafar, Effect of reinforcement corrosion on bond strength, Constr. Build. Mater. 10 (2) (1996) 123–129.
[8] L. Clark, M. Saifullah, Effect of corrosion on reinforcement bond strength, in: Proceedings of the Conference on Structural Faults & Repair, 1993, pp. 113–119.
[9] C. Alonso, C. Andrade, J. Rodriguez, J. Diez, Factors controlling cracking of concrete affected by reinforcement corrosion, Mater. Struct. 31 (1998) 435–441.
[10] T. Vidal, A. Castel, R. François, Analyzing crack width to predict corrosion in reinforced concrete, Cem. Concr. Res. 34 (1) (2004) 165–174.
[11] T. Söylev, R. François, Quality of steel–concrete interface and corrosion of reinforcing steel, Cem. Concr. Res. 33 (9) (2003) 1407–1415.
[12] H. Yalciner, O. Eren, S. Sensoy, An experimental study on the bond strength between reinforcement bars and concrete as a function of concrete cover, strength and corrosion level, Cem. Concr. Res. 42 (5) (2012) 643–655.
[13] H. Lee, T. Noguchi, F. Tomosawa, Evaluation of the bond properties between concrete and reinforcement as a function of the degree of reinforcement corrosion, Cem. Concr. Res. 32 (8) (2002) 1313–1318.
[14] J. Cabrera, P. Ghoddousi, Effect of reinforcement corrosion on the strength of steel concrete bond, in: Proceedings of the International Conference on Bond in Concrete, 1992, pp. 10.11–10.24.
[15] D. Coronelli, Bond of corroded bars in confined concrete: test results and mechanical modelling, Stud. E Richerche 18 (1997) 137–211.
[16] K. Stanish, Corrossion Effects on Bond Strength in Reinforcement in Concrete, University of Toronto, 1997.
[17] G. Mancini, F. Tondolo, Effect of bond degradation due to corrosion – a literature survey, Struct. Concr. 15 (3) (2014) 408–418.
[18] P. Gambarova, G. Rosati, B. Zasso, Steel-to-concrete bond after concrete splitting: test results, Mater. Struct. 22 (1) (1989) 35–47.
[19] L. Marsavina, K. Audenaert, G. De Schutter, N. Faur, D. Marsavina, Experimental and numerical determination of the chloride penetration in cracked concrete, Constr. Build. Mater. 23 (2009) 264–274.
[20] B. Šavija, E. Schlangen, J. Pacheco, R. Polder, Modified Wedge Splitting Test (MWST) – a simple tool for durability investigations of reinforcement corrosion in cracked concrete, in: Concrete Repair, Rehabilitation and Repair III, 2012, pp. 386–391.
[21] M. Ismail, A. Toumi, R. François, R. Gagné, Effect of crack opening on the local diffusion of chloride in cracked mortar samples, Cem. Concr. Res. 34 (2004) 711–716.
[22] A. Djerbi, S. Bonnet, A. Khelidj, V. Baroghel-Bouny, Influence of traversing crack on chloride diffusion into concrete, Cem. Concr. Res. 38 (2008) 877–883.
[23] European Committee for Standardization, EN 1992-1-1 Eurocode 2: Design of concrete structures – Part 1–1: General rules and rules for buildings. European Committee for Standardization, 2004.
[24] T.C. Rilem, Bond test for reinforcing steel: 2. Pull-out test, Mater. Struct. 3 (15) (1970) 175–178.
[25] P. Desnerck, G. De Schutter, L. Taerwe, Bond behaviour of reinforcing bars in self-compacting concrete: experimental determination by using beam tests, Mater. Struct. 43 (S1) (2010) 53–62.
[26] F. de Almeida Filho, M. El Debs, A. de C El Debs, Bond-slip behavior of self-compacting concrete and vibrated concrete using pull-out and beam tests, Mater. Struct. 41 (6) (2007) 1073–1089.
[27] A. Windisch, A modified pull-out test and new evaluation methods for a more real local bond-slip relationship, Mater. Struct. 18 (105) (1985) 181–184.
[28] R. Tepfers, A Theory of Bond Applied to Overlapped Tensile Reinforcement Splices for Deformed Bars, 2nd ed., Chalmers University of technology, Goteborg, 1976.
[29] European Committee for Standardization, EN 197-1:2011 – Cement – Part 1: Composition, specifications and conformity criteria for common cements. Brussels, Belgium: European Committee for Standardization, 2011.
[30] C. Zhang, I. Moore, Nonlinear mechanical response of high density polyethylene. Part I: experimental investigation and model evaluation, Polym. Eng. Sci. 37 (2) (1997) 404–413.
[31] European Committee for Standardization, EN 12390–6:2009 – Testing hardened concrete. Tensile splitting strength of test specimens. Brussels, Belgium: European Committee for Standardization, 2009.